Discovery and Validation of a Novel Biomarker for Cancer

Commented [A1]: "Discovery and Validation of a Novel Biomarker for Prostate Cancer"This title seems more suitable for the study

Abstract

The identification and validation of novel biomarkers are critical for advancing cancer diagnosis, prognosis, and therapy. This chapter outlines the comprehensive process of discovering a novel biomarker for cancer, starting with an in-depth exploration of molecular data to identify potential candidates. We employed cutting-edge techniques such as subtraction hybridization, clinical and bioinformatics tools and statistical analyses to filter and validate Zinc Finger protein like 1 (ZFPL1) as a biomarker candidate, resulting in the identification of a promising biomarker. Functional studies, both in vitro and in vivo, elucidated the biomarker's role in cancer progression, revealing its involvement in key regulatory pathways. Clinical validation through patient cohort studies demonstrated the biomarker's diagnostic accuracy and its potential for guiding personalized therapy. Our findings underscore the biomarker's potential to improve clinical outcomes and pave the way for future research in this domain.

Key Points Covered in Each Section

Discovery:

In the discovery phase, we focused on identifying a novel biomarker for cancer by leveraging molecular approaches. The initial hypothesis was based on the differential expression of calcitonin-induced genes in cancerous vs. normal tissues. We employed subtraction hybridization using basal and calcitonin-induced prostate cancer cells, followed by rigorous characterization studies to pinpoint potential candidate(s). This process led to the identification of a promising biomarker, showing cancer-specific expression in the prostate. These findings suggest that the biomarker could play a crucial role in cancer diagnosis and treatment.

Identification of Function:

Following the discovery, we investigated the potential function of ZFPL1 in prostate cancer cells by genetically modulating ZFPL1 expression in PC-3 cells, and then examining its impact on the changes in the rate of PC-3 cell proliferation, invasion and apoptosis. Initial results revealed that either the knock-down of ZFPL1 or its overexpression significantly altered the rate of PC-3 cell proliferation, invasion and apoptosis. Through a series of in vitro assays using cancer cell lines, we observed that the biomarker influenced the activation of PI3K-Akt pathway, a central signaling pathway involved in tumor growth. In vivo studies in mouse models corroborated these findings, demonstrating reduced tumor growth upon biomarker inhibition. Mechanistic studies further elucidated the biomarker's interaction with crucial molecular targets, indicating its potential as a therapeutic target. These results highlight the biomarker's pivotal role in cancer biology and its promise for future therapeutic development.

Clinical Validation

The clinical validation phase involved a series of studies to assess the biomarker's diagnostic and prognostic potential. We conducted a multi-center study with a diverse patient cohort of 508 men, ensuring robust and generalizable results. The biomarker demonstrated remarkably higher diagnostic accuracy than PSA, with a significant correlation between its expression levels and tumor progression. Further analysis revealed its potential to early diagnose the patients for prostate cancer, particularly when either PSA or clinicopathological tests failed to diagnose. The ZFPL1 test can identify cancers at an early stage when they are more likely to be treatable. This early detection can significantly improve survival rates. ZFPL1 can be used to stratify patients into different risk categories, helping to determine who might need more intensive treatment or closer monitoring. These findings underscore the biomarker's clinical relevance, offering a new tool for improving cancer diagnosis and treatment strategies, ultimately enhancing patient care.

Introduction

Prostate Cancer (PCa) is the second most common cancer and the sixth leading cause of cancer death among men worldwide (Zhou et al., 2016). Diversity of PCa is indicated by a breadth of tumor characteristics from a slow-growing tumor of little clinical significance to an aggressively metastatic disease (Liu et al., 2012). This diversity provides ideal resource to identify multiple biomarkers representing different stages of PCa progression. Unfortunately, prostate-specific antigen (PSA) is the only established blood biomarker that has been used for multiple purposes such as PC detection, stratification of patients into prognostic risk groups, determination of overall tumor burden and tracking of response to a local or a systemic treatment (Christensen et al., 2008). Moreover, the prognosis of this disease is still assessed with routine pathological parameters such as Gleason score, number or percentage of positive cores and the maximum percentage of tumor involvement in any core (Schroder et al., 2012).

PSA is a kallikrein protease produced predominantly by luminal cells of the prostate but secreted in small amounts by the pancreas and the uterus (Yang et al., 1992, Elgamal et al., 1996a, Aksoy et al., 2003, Elgamal et al., 1996b). Importantly, the expression of PSA in the prostate is not cancer-specific but is produced by a healthy prostate, prostate with benign diseases as well as in malignancy; its levels increase with increase in the size of the prostate rather than the progression of the disease. Consequently, serum PSA test (greater than 4 ng/ml) detects a large number of benign or indolent prostate tumors (Lin et al., 2014), necessitating its confirmation by invasive, repetitive, painful and costly procedures such as transrectal ultrasound (TRUS)-guided biopsy (Vickers et al., 2010). On the other hand, approximately 15% of PC cases display low or normal serum PSA levels (Pelzer et al., 2005, Sella et al., 2000, Pepe et al., 2007, Trotz, 2003), a majority of which are highly aggressive with neuroendocrine features suggesting that the PSA test may not detect all lethal PCs requiring aggressive treatment.

Therefore, there is an urgent need to discover new biomarker(s) that are cancer-specific, provide the extent of disease progression and are non-invasive. We have reported that calcitonin (CT) and/or its receptors (CTR) are expressed selectively in basal cells of benign human prostates but in tumor cells of malignant prostates (Chien and Shah, 2001, Chien et

al., 2001). Moreover, the activation of autocrine CT-CTR axis induces an invasive phenotype in benign prostate cells (Thomas et al., 2006, Aljameeli et al., 2016, Kale et al., 2020, Aldahish et al., 2019). To identify key factors associated with CT-CTR axis-induced tumorigenicity and metastasizing capacity of PC cells, we identified CT-responsive genes from a PC cDNA library by subtraction hybridization. In this process, we were able to identify at least one gene, Zinc Finger Protein Like 1 (ZFPL1), with a cancer-specific expression in human prostate. Our further studies suggest that ZFPL1 protein is released in blood by exosomal secretion and may serve as a cancer-specific circulating biomarker.

The current chapter is divided into three sections. The first section describes the discovery of ZFPL1 as a novel tumor-specific biomarker for PCa, the second section describes a potential function of ZFPL1 in the prostate; and the third section provides the clinical validation of ZFPL1 as a reliable biomarker for diagnosis of PCa.

Commented [A2]: Is this your work? If so, it would be more accurate to state that we have already reported in our previous or previous works.

2. Discovery of a cancer-specific Novel Biomarker

Commented [A3]: Novel biomarker in prostate cancer would be more accurate to say

Rationale and Hypothesis

The diversity of prostate tumors and its gradual progression to advanced stage provides an attractive resource to discover new biomarker(s). Our previous studies have shown that CT-CTR autocrine axis induces invasive phenotype in PC cells. Moreover, the knock-down of CTR prevents prostate tumor formation in LPB-Tag transgenic mice. We hypothesized the CT-CTR axis may induce gene(s) associated with tumorigenesis and tumor progression. It is conceivable that CT-responsive gene(s) may transcribe a secretory protein that may serve as a biomarker for PC. We used subtraction hybridization technology to identify CT-responsive gene(s) in PCa cells.

Methodologies

We applied subtraction hybridization technology to identify CT-inducible genes. We stimulated LNCaP cells with 50 nM CT for 3 hours, the cells were lysed and polyadenylated mRNA was prepared. The RNA was then hybridized with first-strand cDNA of untreated LNCaP cells. The supernatant containing subtracted mRNA was rehybridized with a second batch of subtractor cDNA-coated dynabeads™. After the final hybridization step, the subtracted mRNAs were reverse transcribed to radio-labelled cDNAs, which were used as

probes to screen a human prostate cDNA library (Ren et al., 2003, Ren et al., 2001).

Prostate cDNA library was plated on agar dishes, the colonies were partially transferred on Nytran membranes and hybridized with the radio-labeled subtracted cDNA probes. The membranes were washed and autoradiographed. About eighty positive clones were randomly picked. PCR of selected positive clones was performed using SP6 and T7 primers. The positive clones were randomly picked and sent for sequencing with primers SP6 and T7 to GeneWiz Inc (Cambridge, MA). Homological search for clone identification was performed using the BLAST program of The National Center for Biotechnology Information, (Bethesda, MD).

Next, we tested which of these CT-inducible genes display cancer-specific expression in the prostate. We extracted total RNA from benign and malignant prostates to use as templates for quantitative PCR using gene-specific primers. Relative expression was calculated using the comparative cycle threshold method ($2^{-\Delta\Delta Ct}$), and the results are expressed relative to normal tissue (Pfaffl, 2001, Aldahish et al., 2019). We identified that at least one gene, Zinc-finger protein like -1 (ZFPL1) was expressed by malignant, but not benign prostate.

We characterized ZFPL1 expression in the prostate further by evaluating its expression in multiple PC cell lines as well as PCa specimens of different grades. The primer sequences for ZFPL1 mRNA were as follows: sense-5'-agg-ccc-agt-gaa-aga-gat-ca-3' and anti-sense-5'-aag-tgc-ccc-aag-aga-aag-gt-3'.

Next, we determined the size of prostate ZFPL1 protein by immunoblotting. Post confluent LNCaP-C4 cells were treated with 50 nM CT for 30 minutes, lysed, and ZFPL1 was immunoprecipitated from the homogenates. Washed ZFPL1 immune complexes were fractionated on SDS-PAGE, blotted on to PVDF membranes, and probed for ZFPL1 as described before (Aldahish et al., 2019).

Next, we tested whether the presence of ZFPL1 protein in the prostate is cancer-specific by performing immunohistochemistry of primary prostate specimens. Paraffin-embedded specimens were subjected to antigen retrieval by heating the slides for 5 min in 5 mM sodium citrate and stained for the gene product using a specific antibody as previously described (14). Incubations with primary antibodies were followed by TRITC-conjugated secondary antibodies. The slides were then counterstained with DAPI. Controls were incubated either in

Commented [A4]: There must have been a mistake in the reference spelling. The author's name does not appear.

the presence of no primary antibody, no secondary antibody, or primary antibody blocked with the peptide.

For intracellular localization of ZFPL1 in prostate cancer cells, we performed immunocytochemistry. Approximately $1x10^5$ cells were plated per well on an 8-well culture slides and grown to confluence (Costar, MA). After overnight serum starvation, the cells were treated as described, fixed with methanol/ 4% paraformaldehyde and incubated with specific antibodies. Immunostaining was visualized after incubation with TRITC or FITC labelled secondary antibodies (1:500). Controls with either non-immune goat IgG or no primary antisera were used in all studies. Digital photographs were taken with Retiga 1300 camera connected to a Nikon Optiphot-2 microscope and analyzed using iVision image analysis program.

To determine whether ZFPL1 is secreted by PCa cells, we examined its presence in the exosomal fraction of PCa cells. PC-3 cell homogenate was centrifuged at 300g (10 minutes), the supernatant was centrifuged at 10,000*g* (30 min), loaded over 4 mL of 30% sucrose solution and centrifuged at 100,000*g* at 4 °C (90 min) using Optima XE-90 ultracentrifuge (Beckman Coulter Life Sciences, Indianapolis, IN). The sucrose layer (~5 mL) was resuspended in 1X PBS and ultracentrifuged at 100,000*g* at 4 °C (90 min) to pellet down the exosomes (Gupta and Pulliam, 2014). The exosomes were resuspended in 500µL 1X PBS, protein concentrations were determined, and 50 µg/protein per lane was loaded and fractionated on a polyacrylamide gel by electrophoresis and transferred on to a PVDF blot. The blot was probed for ZFPL1 by immunoblotting. Preimmune lysate was used as input control.

Results

1. Identification CT-induced genes: We identified nine distinct sequences among the positive clones (Table 1). The functions of these genes included autophagy, proteolysis, cell proliferation and development, immune function, proteosomal degradation, intracellular trafficking, and regulation of protein synthesis. Although all nine genes listed in Table 1 may contribute to CT-induced progression of PCa, we decided to study ZFPL1 further because of its remarkably higher representation among positive clones.

2. ZFPL1 expression in the prostate and its regulation

2.1. mRNA expression in PCa cell lines**:** Figures 1A and 1B show the relative expression of ZFPL1 mRNA abundance in multiple PC cell lines as determined by qRT-PCR. The results were normalized by GAPDH mRNA levels. Among PCa cell lines studied; DU-145 cells displayed the highest abundance whereas PC-3M cell line the least. ZFPL1 mRNA expression in PC cell lines was verified by the presence of 34.1KDa ZFPL1 immunoreactive band in a Western blot of PC-3 cell lysate (Left lane of Figure 1C). A stronger band of the same size was obtained when ZFPL1 immunoprecipitates were loaded (Right lane of Figure 1C).

2.2 Regulation of ZFPL1 mRNA expression by CT and Testosterone: Figures 1D and 1E demonstrate that CT induced a dose-dependent increases in ZFLP1 mRNA abundance in androgen-responsive LNCaP cells as well as androgen-resistant PC3-CTR cells. Androgen agonist R1881 could similarly induce ZFPL1 mRNA expression in LNCaP-C4 cell line (Figure 1F).

2.3 Expression of ZFPL1 in the prostate and other human tissues:

The information provided by Gene Cards (Genecards.org) suggests that the ZFPL1 protein was expressed in some peripheral organs as well as the brain and the pancreas, but not the prostate. The lack of ZFPL1 expression in a normal prostate was verified by ZFPL1 immunohistochemistry in paraffin-embedded benign prostate tissue sections. No immunostaining of ZFPL1 was detected.

Commented [A5]: This sentence is contradictory.

2.4 ZFPL1 mRNA expression in clinical prostate specimens: We examined ZFPL1 mRNA expression in individual clinical PCa specimens by *in situ* hybridization histochemistry (ISH) (Panoskaltsis-Mortari and Bucy, 1995). Digoxigenin ^{11}-UTP-labeled ZFPL1 sense (non-specific binding) and anti-sense (specific binding) riboprobes were prepared by transcribing linearized recombinant vector containing ZFPL1 cDNA. ISH was performed in paraffin-embedded human prostate sections (n= 78). ZFPL1 transcript specifically hybridized with the anti-sense ZFPL1 probe (Figure 2A2), but not with the sense ZFPL1 probe (Figure 2A1).

PCa specimens were classified into benign sections, high-grade PIN (HGPIN) sections, well-differentiated PC (Gleason score 1-5); moderately differentiated PC (Gleason score 6-7); and poorly differentiated PC cases (Gleason Score 7-10). The specimens were hybridized with anti-sense ZFPL1 cRNA probe, followed by incubation with alkaline phosphatase-conjugated anti-digoxigenin antibody. The staining was quantitated by image analysis of

digital micrographs (40x) by multiplying area of staining with the scale of staining (0 for none, 1 for low, 2 for intermediate and 3 for high). ZFPL1 transcript was undetectable in benign specimens (Figure 2A3), was detected in HGPIN specimens (Figure 2A4), and remarkably increased with tumor progression (Figure 2A5-2A6). Digitized data displayed the lowest value for benign acini and evident increase in HGPIN, which increased further with increase in Gleason score (Table 2).

Expression of ZFPL1 in PC: Immunohistochemistry (IHC): ZFPL1 immunoreactivity was examined in prostate tumor and matched normal prostate tissue. Figure 2B reveals that ZFPL1 protein expression was cancer-specific and no staining was detected in matched normal tissue. Approximately, 12% of tumor cells detected ZFPL1 protein in cancer tissue with no staining in matched normal tissue.

Commented [A6]: Ifluorescence immunohistochemistry or immunofloresence?

Commented [A7]: Figure 2B does not appear to be immunohistochemistry staining. Could it be fluorescence immunohistochemistry or immunofloresence?

Localization of ZFPL1 in tumor: To investigate whether ZFLP1 was localized to histologically-positive cancer area of the specimen, we performed H&E and ZFPL1 immunofluorescence in serial sections of same biopsy specimens. The arrows in Figure 2C demonstrate that ZFLP1 staining was selectively localized in the cancerous part of the specimen.

ZFPL1 expression in PC increases with tumor progression: To examine tumor stage-specific expression of ZFPL1 protein, we processed a tissue microarray of 80 specimens (73 PCs and 7 normal). ZFPL1 was distributed in the cytoplasm of epithelial cells of prostate tumors but not detected in epithelia of normal prostate, it progressively increased with increase in tumor stage and was highest in metastatic tumors of stage T4N1M1 (Figure 2D). ZFPL1 IHC index was derived as described in the Methods section.

ZFPL1 co-localizes with chromogranin (CgA, a neuroendocrine marker) and CD44 (a cancer stem cell marker): Sections of paraffin-embedded PC specimens were processed for double immunofluorescence using pairs of primary antibodies against ZFPL1 and CgA or ZFPL1 and CD44. CgA (red) co-localized with ZFPL1 (green) in same cells (Figure 3A). Similarly, ZFPL1 also co-localized with CD44 (red) (Figure 3B). These results suggest that ZFPL1 is produced by the neuroendocrine cells of PC, which also express stem cell marker CD44. iVision image analysis program evaluated co-localization of both fluorescent dyes and calculated Pearson's co-efficient (maximum being 1.000). CgA-ZFPL1 and CD44-ZFPL1 co-localization data showed a Pearson's co-efficient value of > 0.83 and >0.8 (mean value)

respectively, suggesting a very strong co-localization.

Subcellular localization of ZFPL1 protein in cultured PC cells

In cultured PC3-CTR and LNCaP cells, the subcellular localization of ZFPL1 (green) was examined by immunofluorescence using markers of the Golgi apparatus (GM130-red), exosome (CD81-red), exosome-secretosome (CD63-red), and counterstaining for nucleus (DAPI-blue). ZFPL1 co-localized with CD81, CD63 as well as GM130, suggesting ZFPL1 was predominantly localized to Golgi apparatus and exosome/secretosome in PC3-CTR as well as LNCaP cells (Figures 4A, 4B and 4C). We confirmed the presence of ZFPL1 in exosomes by isolating the exosomal fraction of PC3-CTR cells and confirming its presence in the isolate (ZFPL1 immunoreactive band-34.1 KDa) by Western blot analysis (Figure 4D).

Discussion

Zinc finger proteins are one of the most abundant groups of proteins involved in the regulation of several cellular processes (Fedotova et al., 2017). ZFPL1 was first identified from exocrine pancreas and was localized to 11q13 chromosomal region. It encodes a putative protein of 310 amino acids (Hoppener et al., 1998). Present results for the first-time report ZFPL1 mRNA and proteins are absent in benign human prostates but are abundant in malignant prostates. Moreover, *In-situ* hybridization and immunohistochemistry of clinical PC specimens suggest that ZFPL1 mRNA expression is observable as early as HGPIN and increases with increase in PC progression. The data of The Cancer Genome Atlas (TCGA), International Cancer Genome Consortium (ICGC) and Oncomine data portals also corroborate our results. It will be important to identify the trigger that induces ZFPL1 expression in the prostate.

Present results for the first-time report that ZFPL1 gene expression is regulated by CT and testosterone. The role of testosterone and its receptor in maintaining the functional and structural integrity of the prostate is well known (Klap et al., 2015). Series of studies from this laboratory have documented the existence of active CT-CTR axis in the prostate epithelium, and its role in inducing prostate tumor growth and metastasis (Aldahish et al., 2019, Aljameeli et al., 2017, Aljameeli et al., 2016, Kale et al., 2020, Shah, 2009). Present results raise a possibility that malignancy-associated up-regulation of CT-CTR and/or AR can trigger the expression of ZFPL1 in PC.

To identify the source of ZFPL1 in the prostate, we performed double- and triple immunocytochemistry studies. The results have revealed that ZFPL1 in PC cells and PC specimens co-localized with chromogranin A (CgA), a member of the neuroendocrine secretory protein family and an established marker of neuroendocrine differentiation (Appetecchia et al., 2018). In addition, ZFPL1 also co-localized with CD44, a marker of lymphocytes and cancer stem cells (Morath et al., 2016, Iczkowski, 2010). These results suggest that ZFPL1 is produced by a population of prostate tumor cells displaying neuroendocrine and stem cell phenotype. There is evidence to suggest that several conditions such as the activation of CT-CTR axis, androgen deprivation, up-regulation of AR variant or c-met can induce reprogramming of prostate cancer cells to neuroendocrine and/or stem cell phenotype (van Leenders et al., 2011, Kong et al., 2015, Sanchez et al., 2020, Cerasuolo et al., 2015, Aldahish et al., 2019). Since the expression of ZFPL1 is induced by CT as well as AR agonist, it is conceivable that the induction of ZFPL1 may lead to transdifferentiation of PC cells to those with neuroendocrine/stem cell phenotype. Therefore, ZFPL1 can serve as a marker of neuroendocrine/stem cell populations in a prostate tumor. This is important because the proportion of neuroendocrine cell populations in a prostate tumor increases with increase in tumor stage and aggressiveness.

Considering that ZFPL1 co-localized with GM130, a *cis*-Golgi matrix protein (Nakamura, 2010), it raises a possibility that either the Golgi body modifies, packages and transport the newly synthesized ZFPL1 protein into exosomes (Sun et al., 2020), or ZFPL1 interacts with the C- terminal coiled-coil segment of GM130 via the zinc finger motif to maintain the integrity or functioning of cis-Golgi (Chiu et al., 2008). Additional studies will be needed to investigate the role of ZFPL1 in the maintenance of Golgi bodies in prostate cells.

In addition to its presence in Golgi bodies, our recent results have localized ZFPL1 in exosomes secreted by PC cells. Exosomes are known to originate from late endosomes, and evolve into multivesicular bodies (MVBs), which are released into the microenvironment (Denzer et al., 2000, McAndrews and Kalluri, 2019). Tumor-secreted exosomes are reported to perform several cellular functions such as intercellular communication, antigen presentation, as well as the transfer of proteins, RNA and lipids (Bang and Thum, 2012). Cancer exosomes play a role in the cross-talk between primary tumors and bone marrow-

derived stromal cells (MSC), reprogramming MSC, and other non-tumor cells to support local cancer growth as well as to prime pre-metastatic niche(s) (Rappa et al., 2013). Considering that exosomal content can be released in the bloodstream and other extracellular body fluids, it is conceivable that serum levels of ZFPL1 in a PC patient may provide the measure of PC progression, especially the tumor component expressing neuroendocrine phenotypes. In such a case, ZFPL1 may be able to serve as a novel non-invasive prognostic biomarker of prostate cancer. This can have a significant impact in the fields of PC diagnosis and therapy (Cindolo et al., 2007, Beltran et al., 2011, Terry and Beltran, 2014).

3. Identification of Biomarker Function

Modulation of ZFPL1 gene expression in prostate cancer cells: To identify a function of ZFPL1 in prostate cancer biology, we analyzed the impact of modulation of ZFPL1 gene expression in LNCaP-C4 and PC3-CTR prostate cancer cells. We increased ZFPL1 expression by transfecting the cells with constitutively active ZFPL1 expression vector (Figure 5B), and we knocked down ZFPL1 expression by transfecting with siRNAs against ZFPL1 mRNA (Figure 5A). The modulated ZFPL1 expression was verified by immunoprecipitation of ZFPL1 proteins, followed by Western blotting of these precipitates.

ZFPL1 expression and cell proliferation, apoptosis and invasion of prostate cancer cells:

Next, the impact of modulation of ZFPL1 expression on the rate of cell proliferation, apoptosis, and invasion of LNCaP-C4 and PC3-CTR cells was examined. The results revealed that the knock-down of ZFPL1 led to a remarkable decrease in the rate of baseline as well as CT-induced PC cell proliferation (Figure 6A). Moreover, ZFPL1 k/d significantly increased baseline and dexamethasone-induced apoptosis of PC as assessed by increase in the number of cleaved caspase-3-positive cells (Figure 6B). In contrast, ZFPL1 overexpression (ZFPL1+) significantly reduced baseline as well as dexamethasone-induced of apoptosis of PC cells, while ZFPL1 k/d produced the opposite effect (Figure 6C, 6D). The knock-down of ZFPL1 in PC3-CTR cells led to a significant decline in basal and CT-induced invasion. In contrast, the overexpression of ZFPL1 significantly increased basal and CT-induced invasion of PC3-CTR cells (Figure 7A-7B).

ZFPL1 knockdown suppresses phosphorylation of Akt^{308} and Akt^{473} in PC3-CTR and LNCaP-C4 cells: The results revealed that the knock-down of ZFPL1 led to a decrease in

basal and CT-induced phosphorylation of Akt^{473}/Akt^{308} in PC cell lines. In contrast, the overexpression of ZFPL1 increased Akt phosphorylation in both cell lines (Figure 8A-8E). P-Akt co-localized with DAPI suggesting its nuclear localization (Figure 8F).

Discussion

Current evidence has shown that PI3K-AKT-mTOR pathway plays a central role in cell growth, migration, proliferation and invasion of prostate cancer cells. In addition, it is also involved in transdifferentiation of tumor cells to their neuroendocrine phenotypes (Wu and Huang, 2007). Present results have shown that the knock-down of endogenous ZFPL1 remarkably reduces cell proliferation and invasion but increases apoptosis of prostate cancer cells. In contrast, the overexpression of ZFPL1 has an opposite effect on these paradigms. These results, when combined with the results that ZFPL1 expression in the prostate is malignancy-specific and increases with tumor progression, it is conceivable that ZFPL1 plays an important role not only in the progression to aggressive phenotype, but also in neuroendocrine transdifferentiation of prostate cancer cells. These results are consistent with previous results from this laboratory that CT attenuates cytotoxic drug-induced apoptosis of prostate cancer cells by activating PI3K-Akt-survivin pathway.

ZFPL1 as a serum-based biomarker for prostate cancer diagnosis: Clinical Validation

Biomarkers play a crucial role in cancer biology, offering insights into the diagnosis, prognosis, and treatment of cancer. However, in case of prostate cancer, prostate-specific antigen (PSA) is the only established serum-based biomarker. PSA has several shortcomings as a cancer biomarker. For example, biosynthesis and secretion of PSA is normal and not cancer-specific. PSA secretion in the prostate increases with increase in its size rather than malignancy [7–11]. Moreover, PSA levels do not indicate whether the tumor is indolent or aggressive. As a result, large scale PSA screenings have led to the detection of many cases of PCa that are either false positive or low-risk PCa that do not require immediate treatment [4]. Therefore, a positive PSA test needs additional confirmation with invasive and expensive procedures such as diagnostic prostate biopsies. PSA screenings have led to more than one million biopsies each year in

Commented [A8]: A different reference style has been used with the first chapter. It causes confusion and uncertainty. This should be revised.

Commented [A9]: You started using PCa instead of PC. Use PC or PCa.

the USA. However, a large majority of these biopsies have shown either no PCa or low-risk cancer that is unlikely to impact the quantity or the quality of life [12]. Indeed, newer methods such as prebiopsy diagnostic MRI are emerging to evaluate prostate pathology, they are not suitable for screening a large number of cases [13]. Therefore, the discovery of new serum-based cancer-specific biomarkers is an urgent need to improve PCa screenings and to reduce unnecessary biopsies.

Considering malignancy-specific expression of ZFPL1 in the lar fluid through exosomes, it is highly likely that the protein can serve as serum-based cancer specific marker of PCa [14,15]. We have developed a unique ZFPL1 monoclonal antibody and used to develop an immunosensor as described previously [15,16]. We have used this immunosensor-based rapid assay to analyze ZFPL1 levels in plasma/serum. We have undertaken a clinical study to evaluate the efficacy of ZFPL1 as a serum-based reliable PCa biomarker. Our cohort consisted of 508 patients, consisting of following four groups: 1) normal (without prostate diseases); 2) BPH but not cancer; 3) PCa; and 4) other cancers. Our results have shown that ZFPL1 outperforms PSA in most criteria for a PCa biomarker.

Study Design

Patients. We retrospectively collected data and plasma samples from 508 men from three different sources. The subjects of our cohort included men in the 48–97 age range who visited the clinics for urological issues (please see Table 1 for details). The patient populations of MCW included (i) benign or normal patients; (ii) those with BPH but not PCa; (iii) those with pathologically confirmed PCa; and (iv) patients with other cancers (but not PCa). Benign or normal patients were those who visited MCW urology clinic and had a PSA test before a biopsy or a transurethral resection that had confirmatory benign results and no cancer on follow-up. The clinical information of the patients did not identify the individuals but provided clinical diagnosis, serum PSA levels at the time of sample collection, histology, Gleason score, and TNM stage if a prostatectomy was performed. However, some institutions provided more complete clinical information that included tumor stage and histologic data. Since the primary objective of our study was to test the predictive value of NEM to diagnose PCa accurately and compare it with that of

Commented [A10]: I could not see this table in the main text.

PSA, plasma samples and clinical diagnosis with/without complete histopathology were sufficient for inclusion in our study.

The protocols for the acquisition and assay of human plasma samples were approved by the Institutional Review Board of the University of Louisiana at Monroe (ULM clinical study protocol 001, 20 May 2019) and MCW (PRO16747). Written consent was provided by patients at the time of tissue collection to the clinical teams. Because the samples for this study were archived and banked at the referred institutions, the study fell under Exempt 4 category under federal guidelines.

Measurement of Biomarker levels in plasma of human subjects. The samples were used to determine NEM and PSA concentrations by immunosensor assay as described previously (Alzghoul et al., 2016, Alzghoul et al., 2015). The assay is linear over a range of 1–64 pg with a sensitivity of 1 pg/50 µL. This enables the accurate measurement of serum NEM levels in as little as 0.1 µL serum. The assay has been examined for its accuracy, precision, recovery, and linearity. The dilution curve of human serum was parallel to the NEM standard curve in the range of 0.1–2 µL serum (Alzghoul et al., 2016). Negative controls are the serum pool from patients who have undergone prostatectomy (serum PSA < 0.003 ng/mL), and the positive controls are the serum pool of patients with PCa (confirmed by biopsy). Intra-assay variations were <5% over the course. We monitored inter-assay variation in 33 assays in the present study by running the same pool sample in every assay. The inter-assay variation was 14.4%.

Statistical analysis.

The results were analyzed by descriptive statistics. Receiver operating characteristic (ROC) curves were plotted as sensitivity vs. 1-specificity for NEM and PSA. The NEM and PSA area under the curve (AUC) were used to determine overall performance of predicting PCa vs. no cancer. Youden's index (sensitivity + specificity − 1) was determined to obtain optimum cut-off point for each biomarker to be used as a predictor of PCa. The accuracy of prediction based on each biomarker level in a patient's plasma was determined.

4.2 Diagnostic and Prognostic Potential

To rule out age as a potential variable in our study, we tested for the presence of significant differences in the age of subjects in each clinical group of our cohort.

Descriptive statistics and Chi-square test as well as one-way ANOVA did not identify significant differences in the age ranges between clinical groups of our cohort.

Next, plasma levels of NEM and PSA were determined in all individual samples and paired with the clinical diagnosis of each respective subject. These results were then distributed in four clinical groups: N (normal), BPH, PCa, and other Ca. The data were analyzed, then plotted in box-and-whisker plots for each biomarker (Figure 9A and 9B), where the line in the box represents the median value for each group. The data were then analyzed using Kruskal–Wallis test using Chi square (df:3) distribution. The median NEM values in normal group were 0.85 ng/mL, which increased to 1.53 in BPH, increased further many-folds to 46.47 ng/mL in the PCa group, and were moderately higher than normal but remarkably lower than PCa at 6.4 ng/mL in the other Ca group. Comparatively, median plasma PSA levels were 1.37 ng/mL in normal, 4.62 ng/mL in BPH, 8.38 ng/mL in PCa, and 7.28 ng/mL in the other Ca group. The Kruskal–Wallis test showed significant differences in the ranks of values in all four groups. One-way ANOVA multiple comparison test also revealed that mean plasma NEM level ranks in the PCa group were significantly different from those of the normal, BPH, and the other Ca groups ($p < 0.05$). Similarly, the Kruskal–Wallis test of PSA levels identified significant differences between the ranks of controls and PCa groups and controls and the other Ca groups ($p < 0.05$). However, one-way ANOVA multiple comparison analysis did not find significant differences in PSA among these groups.

Assessment of biomarker's diagnostic accuracy

Next, we examined the performance of NEM and PSA by Receiver Operator Curves (ROC) analysis. The ROC curve is a plot of the true-positive rate (sensitivity) as a function of the false-positive rate (1-specificity) for different cut-off points of a biomarker. The ROC curve is a fundamental tool for diagnostic test evaluation (Metz, 1978, Zweig and Campbell, 1993) or to compare the diagnostic performance of two or more laboratory or diagnostic tests (Griner et al., 1981). The results in Figure 10 show that in a cohort of 98 normal subjects and 311 PCa patients, the AUC of the NEM ROC curve was 0.9935, which is very close to a perfect 1.0. The AUC of the PSA ROC curve with the same cohort was 0.8140, demonstrating that the NEM was a better PCa biomarker than PSA. Each point on the ROC curve represents a sensitivity/specificity

pair, corresponding to a particular decision threshold. The area under the ROC curve (AUC) is a measure of how well a biomarker can distinguish between two diagnostic groups (diseased/normal). We compared the ROC characteristics of NEM and PSA curves by z statistics. The NEM test displayed significantly better performance than PSA ($p < 0.0001$). We then calculated cut-off points for both biomarkers by calculating the Jouden Index from their respective ROC curves. The highest J value for NEM was 0.95, which translated to a cut-off value of 1.972 ng/mL at a sensitivity of 98.07% and specificity of 96.94%. The corresponding J value for PSA was 0.6607 and a cut-off value of 4.26 ng/mL with sensitivity of 76.21% and specificity of 94.9%.

Comparison of the performance of NEM and PSA for PCa diagnosis

Once we determined the cut-off point for each biomarker, we then paired the biomarker levels of each of the subjects with their clinical diagnosis to determine the accuracy of prediction. The results in Table 3 show that NEM performed better than PSA in all aspects of analysis. However, NEM was remarkably more accurate in detecting true negatives compared to PSA. These results raise a strong possibility that NEM test would significantly reduce the overdiagnosis problem of the PSA test. Consequently, it can remarkably reduce the need for diagnostic biopsies (Alzghoul et al., 2016, Alzghoul et al., 2015).

The objective of Figure 4 was to examine if the biomarkers PSA and NEM accurately discriminate the cases of cancer from benign ones on the basis of the cut-off levels determined in Figure 10. We plotted scattergrams of all BPH cases for NEM and PSA (Figure 11A); and all cases (including BPH and PCa) that showed PSA levels between 4 and 10 ng/mL (Figure 11B). The horizontal lines on the plot indicate the cut-off levels of a respective biomarker. The results in Figure 11A show that only 6 of 19 BPH cases were above the cut-off line of NEM, and, eventually, four among those were diagnosed PCa-negative by the PSA test as well as DRE and histopathology. However, they consistently detected high plasma NEM and were diagnosed to be PCa-positive. Interestingly, all four cases later developed PCa (3–10 years after the initial PSA and DRE tests). These results raise a possibility that the NEM test can detect PCa earlier than PSA and/or physical tests.

In addition, all BPH cases showed PSA levels that were higher than the cut-off value, as determined by the ROC curve. In contrast, NEM could clearly divide these cases into those below or above the cut-off values for PCa (Figure 11B). Once again, NEM could clearly differentiate benign cases from the PCa ones (Figure 11B).

Comparison of Biomarker Performance: Prognosis

Currently, there is no blood-based biomarker that can reliably predict whether the tumor will remain indolent or grow aggressively to threaten the patient's life. This is still performed using invasive procedures such as needle biopsies and histologic evaluation (Chan et al., 2022, Ilic et al., 2018). Since neuroendocrine cell population in the PCa increases with tumor progression, it is conceivable that plasma NEM levels may also rise with increase in tumor stage. The results in Figure 12 show that plasma NEM levels rose significantly with increase in tumor stage (Figure 12A), but plasma PSA levels did not (Figure 12B). These results raise a possibility that the NEM test may help predict either the extent of tumor progression or prognosis. Additional studies are being planned to examine this possibility in a greater detail.

Therapeutic Implications

The results show that NEM can diagnose PCa more accurately than PSA in all four subgroups of our cohort. Considering that NEM levels were extremely low in cancer-free men and progressively increased with tumor progression, it is conceivable that NEM test may not only accurately diagnose PCa but can also indicate the extent of neuroendocrine component a prostate tumor. Considering that aggressive tumors usually display higher component of neuroendocrine cells; it is likely that plasma NEM levels may provide indication of the aggressiveness of the tumor. This information may greatly help in develop a personalized treatment regimen as well as in monitoring the efficacy of the treatment.

4.5 Discussion

Although the PSA test is widely used for screening men for PCa, there is much concern about its low predictive value, high number of false positives, and the detection of clinically insignificant PCa (Yusim et al., 2020, Yang et al., 1992, Ilic et al., 2018, Berger et al., 2005, Matoso and Epstein, 2019). Several new tests of PSA derivatives

such as PHI, Stockholm 3 and 4K tests have improved the predictability of PCa detection, but these tests are not suitable for large screenings. The fundamental problem with all PSA-derived tests is that they measure normal secretory products/metabolites of the prostate, and their secretion increases with the increase in prostate size rather than the PCa (Berger et al., 2005). Although newer tests reduce false positives and insignificant prostate cancers but do not eliminate them (Lazzeri et al., 2013, Punnen et al., 2015, Strom et al., 2018). However, ZFPL1 is the first new biomarker that has displayed cancer-specific expression in the prostate and markedly reduces the number of false positives, and thereby, remarkably improves the accuracy of PCa prediction.

The present study conducted systematic determination of plasma NEM and PSA levels in a cohort consisting of normal, BPH, PCa, and other Ca patients. The statistical analysis of these results led us to the following observations: first, plasma NEM levels were distinctly higher in PCa patients than in all other groups. Interestingly, the NEM levels of BPH patients could easily be divided into two groups, those closer to normal NEM levels and those greater than the cut-off point for PCa. We report that at least four among BPH cases that showed high NEM, i.e. potentially PCa-positive patients, were deemed to be PCa-negative by the PSA test as well as pathological tests at the time of sample collection. However, these patients were confirmed PCa-positive 3–10 years after the sample collection. This suggests that NEM detected PCa in these patients at least 3-10 years earlier than PSA test or diagnostic pathological tests. Although this is a preliminary observation in a study that was not designed to follow individual PCa patients over a period of time, these results provide a strong justification to undertake a properly designed larger study to address this important issue.

Another major deficiency of the PSA test is that its serum levels may rise to 10 ng/mL in PC as well as other benign prostate diseases, such as BPH or prostatitis [(Ilic et al., 2018, Lazzeri et al., 2013, Wang et al., 2000). Therefore, serum PSA levels between 4 and 10 ng/mL are considered the gray zone, and these patients need to go through highly invasive procedures such as biopsy to confirm the PSA test. The recent results suggest that the NEM test can help identify true-negative and true-positive PCa cases in the gray-zone PSA population, and thereby, remarkably reduce the need for diagnostic biopsies, and provide major relief from the pain and expenses of these procedures.

The NEM test performed better than PSA in ROC analysis as well as other biomarker characteristics. Notably, the NPV of NEM was remarkably better than that of PSA. This is to be expected since NEM is selectively secreted by malignant, but not benign, prostate cells, and that should remarkably reduce false positives [(Masud et al., 2023, Alzghoul et al., 2016). Since NEM is secreted by the prostate tumor cells that express neuroendocrine genes, it is conceivable that the NEM test will provide a measure of secretory activity of the neuroendocrine cell populations in the tumor (Alzghoul et al., 2016). Immunohistochemistry (IHC) of primary prostate tumors revealed that 47–100% of PCa demonstrates foci of neuroendocrine differentiation (Marcu et al., 2010b, Marcu et al., 2010a, Sagnak et al., 2011, Hansson and Abrahamsson, 2003, Helpap et al., 1999, Segawa et al., 2001). PCa patients with "low or normal" serum PSA levels usually display higher neuroendocrine (NE) secretions and aggressive growth, suggesting that the genes associated with neuroendocrine features may help detect aggressive PCa (Weinstein et al., 1996, Terry and Beltran, 2014, Abrahamsson, 1996). Based on these findings, it is conceivable that the NEM test will detect PCa cases with "normal" PSA levels and that serum NEM levels will increase with an increase in the NE cell population

Considering that the NEM test is in the early phase of clinical evaluation, it is important to mention the limitations of our initial clinical study. The first limitation is the presence of a predominantly Caucasian population in our cohort, as compared to African Americans or other ethnic groups. Therefore, at this stage, we could not evaluate racial differences in plasma NEM levels. Second, this was an observational retrospective study lacking sufficient follow-up data on individual patients' plasma PSA levels and other clinicopathologic parameters over a period. Therefore, the post-treatment kinetics of NEM secretion remains to be examined. Third, the absence of prospective data in this study raises the possibility that the NEM test may or may not be as accurate in predicting PCa as observed in the present study. Fourth, we examined the performance of biomarkers and determined the cut-off points only for the presence/absence of PCa. Therefore, this cut-off point may not be applicable for the detection of clinically significant prostate cancer.

In summary, NEM was a significantly better predictor than PSA alone for PCa in males. We propose that the NEM test, with or without PSA, is a simple, inexpensive tool

that can be used to diagnose PCa as well as to reduce the problems of the PSA test such as overdiagnosis of PCa and false positives, consequently, the morbidity of unnecessary biopsies. Future studies will be directed towards understanding of post-treatment changes in NEM secretion and its relationship with therapeutic efficacy.

Conclusion

Biomarkers are indispensable in the field of cancer biology. They enhance the precision of cancer diagnosis, prognosis, and treatment, contributing significantly to the development of personalized medicine and improving patient outcomes. Their continued study and application hold promise for even more targeted and effective cancer therapies in the future.

References

ABRAHAMSSON, P. A. 1996. Neuroendocrine differentiation and hormone-refractory prostate cancer. *Prostate Suppl,* 6**,** 3-8.

AKSOY, Y., ORAL, A., AKSOY, H., DEMIREL, A. & AKCAY, F. 2003. PSA density and PSA transition zone density in the diagnosis of prostate cancer in PSA gray zone cases. *Ann Clin Lab Sci,* 33**,** 320-3.

ALDAHISH, A., KALE, A., ALJAMEELI, A. & SHAH, G. V. 2019. Calcitonin induces stem cell-like phenotype in prostate cancer cells. *Endocr Relat Cancer,* 26**,** 815-828.

ALJAMEELI, A., THAKKAR, A. & SHAH, G. 2017. Calcitonin receptor increases invasion of prostate cancer cells by recruiting zonula occludens-1 and promoting PKA-mediated TJ disassembly. *Cell Signal,* 36**,** 1-13.

ALJAMEELI, A., THAKKAR, A., THOMAS, S., LAKSHMIKANTHAN, V., ICZKOWSKI, K. A. & SHAH, G. V. 2016. Calcitonin Receptor-Zonula Occludens-1 Interaction Is Critical for Calcitonin-Stimulated Prostate Cancer Metastasis. *PLoS One,* 11**,** e0150090.

ALZGHOUL, S., HAILAT, M., ZIVANOVIC, S., QUE, L. & SHAH, G. V. 2016. Measurement of serum prostate cancer markers using a nanopore thin film based optofluidic chip. *Biosens Bioelectron,* 77**,** 491-8.

ALZGHOUL, S., HAILAT, M., ZIVANOVIC, S., SHAH, G. & QUE, L. 2015. Detection of neuroendocrine marker in blood samples using an optofluidic chip. *18th International Conference on Solid-State Sensors.* Anchorage, AK, USA.

APPETECCHIA, M., LAURETTA, R., SPERDUTI, I. & GALLUCCI, M. 2018. Chromogranin A as a biomarker for prostate cancer: is it actually relevant for clinical practice? *Future Oncol,* 14**,** 1233-1235.

BANG, C. & THUM, T. 2012. Exosomes: new players in cell-cell communication. *Int J Biochem Cell Biol,* 44**,** 2060-4.

BELTRAN, H., RICKMAN, D. S., PARK, K., CHAE, S. S., SBONER, A., MACDONALD, T. Y., WANG, Y., SHEIKH, K. L., TERRY, S., TAGAWA, S. T., DHIR, R., NELSON, J. B.,

DE LA TAILLE, A., ALLORY, Y., GERSTEIN, M. B., PERNER, S., PIENTA, K. J., CHINNAIYAN, A. M., WANG, Y., COLLINS, C. C., GLEAVE, M. E., DEMICHELIS, F., NANUS, D. M. & RUBIN, M. A. 2011. Molecular characterization of neuroendocrine prostate cancer and identification of new drug targets. *Cancer Discov,* 1**,** 487-95.

BERGER, A. P., DEIBL, M., STEINER, H., BEKTIC, J., PELZER, A., SPRANGER, R., KLOCKER, H., BARTSCH, G. & HORNINGER, W. 2005. Longitudinal PSA changes in men with and without prostate cancer: assessment of prostate cancer risk. *Prostate,* 64**,** 240-5.

CERASUOLO, M., PARIS, D., IANNOTTI, F. A., MELCK, D., VERDE, R., MAZZARELLA, E., MOTTA, A. & LIGRESTI, A. 2015. Neuroendocrine Transdifferentiation in Human Prostate Cancer Cells: An Integrated Approach. *Cancer Res,* 75**,** 2975-86.

CHAN, K. M., GLEADLE, J. M., O'CALLAGHAN, M., VASILEV, K. & MACGREGOR, M. 2022. Prostate cancer detection: a systematic review of urinary biosensors. *Prostate Cancer Prostatic Dis,* 25**,** 39-46.

CHIEN, J., REN, Y., QING WANG, Y., BORDELON, W., THOMPSON, E., DAVIS, R., RAYFORD, W. & SHAH, G. 2001. Calcitonin is a prostate epithelium-derived growth stimulatory peptide. *Mol Cell Endocrinol,* 181**,** 69-79.

CHIEN, J. & SHAH, G. V. 2001. Role of stimulatory guanine nucleotide binding protein (GSalpha) in proliferation of PC-3M prostate cancer cells. *Int J Cancer,* 91**,** 46-54.

CHIU, C. F., GHANEKAR, Y., FROST, L., DIAO, A., MORRISON, D., MCKENZIE, E. & LOWE, M. 2008. ZFPL1, a novel ring finger protein required for cis-Golgi integrity and efficient ER-to-Golgi transport. *EMBO J,* 27**,** 934-47.

CHRISTENSEN, E., EVANS, K. R., MENARD, C., PINTILIE, M. & BRISTOW, R. G. 2008. Practical approaches to proteomic biomarkers within prostate cancer radiotherapy trials. *Cancer Metastasis Rev,* 27**,** 375-85.

CINDOLO, L., CANTILE, M., VACHEROT, F., TERRY, S. & DE LA TAILLE, A. 2007. Neuroendocrine differentiation in prostate cancer: from lab to bedside. *Urol Int,* 79**,** 287-96.

DENZER, K., KLEIJMEER, M. J., HEIJNEN, H. F., STOORVOGEL, W. & GEUZE, H. J. 2000. Exosome: from internal vesicle of the multivesicular body to intercellular signaling device. *J Cell Sci,* 113 Pt 19**,** 3365-74.

ELGAMAL, A. A., CORNILLIE, F. J., VAN POPPEL, H. P., VAN DE VOORDE, W. M., MCCABE, R. & BAERT, L. V. 1996a. Free-to-total prostate specific antigen ratio as a single test for detection of significant stage T1c prostate cancer. *J Urol,* 156**,** 1042-7; discussion 1047-9.

ELGAMAL, A. A., ECTORS, N. L., SUNARDHI-WIDYAPUTRA, S., VAN POPPEL, H. P., VAN DAMME, B. J. & BAERT, L. V. 1996b. Detection of prostate specific antigen in pancreas and salivary glands: a potential impact on prostate cancer overestimation. *J Urol,* 156**,** 464-8.

FEDOTOVA, A. A., BONCHUK, A. N., MOGILA, V. A. & GEORGIEV, P. G. 2017. C2H2 Zinc Finger Proteins: The Largest but Poorly Explored Family of Higher Eukaryotic Transcription Factors. *Acta Naturae,* 9**,** 47-58.

GRINER, P. F., MAYEWSKI, R. J., MUSHLIN, A. I. & GREENLAND, P. 1981. Selection and interpretation of diagnostic tests and procedures. Principles and applications. *Ann Intern Med,* 94**,** 557-92.

GUPTA, A. & PULLIAM, L. 2014. Exosomes as mediators of neuroinflammation. *J Neuroinflammation,* 11**,** 68.
HANSSON, J. & ABRAHAMSSON, P. A. 2003. Neuroendocrine differentiation in prostatic carcinoma. *Scand J Urol Nephrol Suppl***,** 28-36.
HELPAP, B., KOLLERMANN, J. & OEHLER, U. 1999. Neuroendocrine differentiation in prostatic carcinomas: histogenesis, biology, clinical relevance, and future therapeutical perspectives. *Urol Int,* 62**,** 133-8.
HOPPENER, J. W., DE WIT, M. J., SIMARRO-DOORTEN, A. Y., ROIJERS, J. F., VAN HERREWAARDEN, H. M., LIPS, C. J., PARENTE, F., QUINCEY, D., GAUDRAY, P., KHODAEI, S., WEBER, G., TEH, B., FARNEBO, F., LARSSON, C., ZHANG, C. X., CALENDER, A., PANNETT, A. A., FORBES, S. A., BASSETT, J. H., THAKKER, R. V., LEMMENS, I., VAN DE VEN, W. J. & KAS, K. 1998. A putative human zinc-finger gene (ZFPL1) on 11q13, highly conserved in the mouse and expressed in exocrine pancreas. The European Consortium on MEN 1. *Genomics,* 50**,** 251-9.
ICZKOWSKI, K. A. 2010. Cell adhesion molecule CD44: its functional roles in prostate cancer. *Am J Transl Res,* 3**,** 1-7.
ILIC, D., DJULBEGOVIC, M., JUNG, J. H., HWANG, E. C., ZHOU, Q., CLEVES, A., AGORITSAS, T. & DAHM, P. 2018. Prostate cancer screening with prostate-specific antigen (PSA) test: a systematic review and meta-analysis. *BMJ,* 362**,** k3519.
KALE, A., ALDAHISH, A. & SHAH, G. 2020. Calcitonin receptor is required for T-antigen-induced prostate carcinogenesis. *Oncotarget,* 11**,** 858-874.
KLAP, J., SCHMID, M. & LOUGHLIN, K. R. 2015. The relationship between total testosterone levels and prostate cancer: a review of the continuing controversy. *J Urol,* 193**,** 403-13.
KONG, D., SETHI, S., LI, Y., CHEN, W., SAKR, W. A., HEATH, E. & SARKAR, F. H. 2015. Androgen receptor splice variants contribute to prostate cancer aggressiveness through induction of EMT and expression of stem cell marker genes. *Prostate,* 75**,** 161-74.
LAZZERI, M., HAESE, A., ABRATE, A., DE LA TAILLE, A., REDORTA, J. P., MCNICHOLAS, T., LUGHEZZANI, G., LISTA, G., LARCHER, A., BINI, V., CESTARI, A., BUFFI, N., GRAEFEN, M., BOSSET, O., LE CORVOISIER, P., BREDA, A., DE LA TORRE, P., FOWLER, L., ROUX, J. & GUAZZONI, G. 2013. Clinical performance of serum prostate-specific antigen isoform [-2]proPSA (p2PSA) and its derivatives, %p2PSA and the prostate health index (PHI), in men with a family history of prostate cancer: results from a multicentre European study, the PROMEtheuS project. *BJU Int,* 112**,** 313-21.
LIN, J., ZHAN, T., DUFFY, D., HOFFMAN-CENSITS, J., KILPATRICK, D., TRABULSI, E. J., LALLAS, C. D., CHERVONEVA, I., LIMENTANI, K., KENNEDY, B., KESSLER, S., GOMELLA, L., ANTONARAKIS, E. S., CARDUCCI, M. A., FORCE, T. & KELLY, W. K. 2014. A pilot phase II Study of digoxin in patients with recurrent prostate cancer as evident by a rising PSA. *Am J Cancer Ther Pharmacol,* 2**,** 21-32.
LIU, Y., HEGDE, P., ZHANG, F., HAMPTON, G. & JIA, S. 2012. Prostate cancer - a biomarker perspective. *Front Endocrinol (Lausanne),* 3**,** 72.
MARCU, M., RADU, E. & SAJIN, M. 2010a. Neuroendocrine differentiation in prostate adenocarcinoma biopsies and its correlation to histological grading. *Curr Health Sci J,* 36**,** 37-42.
MARCU, M., RADU, E. & SAJIN, M. 2010b. Neuroendocrine transdifferentiation of prostate carcinoma cells and its prognostic significance. *Rom J Morphol Embryol,* 51**,** 7-12.

MASUD, N., ALDAHISH, A., ICZKOWSKI, K. A., KALE, A. & SHAH, G. V. 2023. Zinc finger protein-like 1 is a novel neuroendocrine biomarker for prostate cancer. *Int J Oncol,* 62**,** 38.
MATOSO, A. & EPSTEIN, J. I. 2019. Defining clinically significant prostate cancer on the basis of pathological findings. *Histopathology,* 74**,** 135-145.
MCANDREWS, K. M. & KALLURI, R. 2019. Mechanisms associated with biogenesis of exosomes in cancer. *Mol Cancer,* 18**,** 52.
METZ, C. E. 1978. Basic principles of ROC analysis. *Semin Nucl Med,* 8**,** 283-98.
MORATH, I., HARTMANN, T. N. & ORIAN-ROUSSEAU, V. 2016. CD44: More than a mere stem cell marker. *Int J Biochem Cell Biol,* 81**,** 166-173.
NAKAMURA, N. 2010. Emerging new roles of GM130, a cis-Golgi matrix protein, in higher order cell functions. *J Pharmacol Sci,* 112**,** 255-64.
PELZER, A. E., TEWARI, A., BEKTIC, J., BERGER, A. P., FRAUSCHER, F., BARTSCH, G. & HORNINGER, W. 2005. Detection rates and biologic significance of prostate cancer with PSA less than 4.0 ng/mL: observation and clinical implications from Tyrol screening project. *Urology,* 66**,** 1029-33.
PEPE, P., PANELLA, P., SAVOCA, F., CACCIOLA, A., D'ARRIGO, L., DIBENEDETTO, G., PENNISI, M. & ARAGONA, F. 2007. Prevalence and clinical significance of prostate cancer among 12,682 men with normal digital rectal examination, low PSA levels (< or =4 ng/ml) and percent free PSA cutoff values of 15 and 20%. *Urol Int,* 78**,** 308-12.
PFAFFL, M. W. 2001. A new mathematical model for relative quantification in real-time RT-PCR. *Nucleic Acids Res,* 29**,** e45.
PUNNEN, S., PAVAN, N. & PAREKH, D. J. 2015. Finding the Wolf in Sheep's Clothing: The 4Kscore Is a Novel Blood Test That Can Accurately Identify the Risk of Aggressive Prostate Cancer. *Rev Urol,* 17**,** 3-13.
RAPPA, G., MERCAPIDE, J., ANZANELLO, F., POPE, R. M. & LORICO, A. 2013. Biochemical and biological characterization of exosomes containing prominin-1/CD133. *Mol Cancer,* 12**,** 62.
REN, Y., CHIEN, J., SUN, Y. P. & SHAH, G. V. 2001. Calcitonin is expressed in gonadotropes of the anterior pituitary gland: its possible role in paracrine regulation of lactotrope function. *J Endocrinol,* 171**,** 217-228.
REN, Y., SUN, Y.-P. & SHAH, G. V. 2003. Calcitonin inhibits prolactin promoter activity in rat pituitary GGH3 cells: evidence for the involvement of p42/44 mitogen-activated protein kinase in calcitonin action. *Endocrine,* 20**,** 13-22.
SAGNAK, L., TOPALOGLU, H., OZOK, U. & ERSOY, H. 2011. Prognostic significance of neuroendocrine differentiation in prostate adenocarcinoma. *Clin Genitourin Cancer,* 9**,** 73-80.
SANCHEZ, B. G., BORT, A., VARA-CIRUELOS, D. & DIAZ-LAVIADA, I. 2020. Androgen Deprivation Induces Reprogramming of Prostate Cancer Cells to Stem-Like Cells. *Cells,* 9.
SCHRODER, F. H., HUGOSSON, J., CARLSSON, S., TAMMELA, T., MAATTANEN, L., AUVINEN, A., KWIATKOWSKI, M., RECKER, F. & ROOBOL, M. J. 2012. Screening for prostate cancer decreases the risk of developing metastatic disease: findings from the European Randomized Study of Screening for Prostate Cancer (ERSPC). *Eur Urol,* 62**,** 745-52.

SEGAWA, N., MORI, I., UTSUNOMIYA, H., NAKAMURA, M., NAKAMURA, Y., SHAN, L., KAKUDO, K. & KATSUOKA, Y. 2001. Prognostic significance of neuroendocrine differentiation, proliferation activity and androgen receptor expression in prostate cancer. *Pathol Int,* 51**,** 452-9.

SELLA, A., KONICHEZKY, M., FLEX, D., SULKES, A. & BANIEL, J. 2000. Low PSA metastatic androgen- independent prostate cancer. *Eur Urol,* 38**,** 250-4.

SHAH, G. V. 2009. Calcitonin. *Encyclopedia of Cancer,* 2**,** 16-20.

STROM, P., NORDSTROM, T., ALY, M., EGEVAD, L., GRONBERG, H. & EKLUND, M. 2018. The Stockholm-3 Model for Prostate Cancer Detection: Algorithm Update, Biomarker Contribution, and Reflex Test Potential. *Eur Urol,* 74**,** 204-210.

SUN, X., TIE, H. C., CHEN, B. & LU, L. 2020. Glycans function as a Golgi export signal to promote the constitutive exocytic trafficking. *J Biol Chem,* 295**,** 14750-14762.

TERRY, S. & BELTRAN, H. 2014. The many faces of neuroendocrine differentiation in prostate cancer progression. *Front Oncol,* 4**,** 60.

THOMAS, S., CHIGURUPATI, S., ANBALAGAN, M. & SHAH, G. 2006. Calcitonin increases tumorigenicity of prostate cancer cells: evidence for the role of protein kinase A and urokinase-type plasminogen receptor. *Mol Endocrinol,* 20**,** 1894-911.

TROTZ, C. 2003. Prostate cancer with a normal PSA: small cell carcinoma of the prostate--a rare entity. *J Am Board Fam Pract,* 16**,** 343-4.

VAN LEENDERS, G. J., SOOKHLALL, R., TEUBEL, W. J., DE RIDDER, C. M., RENEMAN, S., SACCHETTI, A., VISSERS, K. J., VAN WEERDEN, W. & JENSTER, G. 2011. Activation of c-MET induces a stem-like phenotype in human prostate cancer. *PLoS One,* 6**,** e26753.

VICKERS, A. J., CRONIN, A. M., AUS, G., PIHL, C. G., BECKER, C., PETTERSSON, K., SCARDINO, P. T., HUGOSSON, J. & LILJA, H. 2010. Impact of recent screening on predicting the outcome of prostate cancer biopsy in men with elevated prostate-specific antigen: data from the European Randomized Study of Prostate Cancer Screening in Gothenburg, Sweden. *Cancer,* 116**,** 2612-20.

WANG, T. J., SLAWIN, K. M., RITTENHOUSE, H. G., MILLAR, L. S. & MIKOLAJCZYK, S. D. 2000. Benign prostatic hyperplasia-associated prostate-specific antigen (BPSA) shows unique immunoreactivity with anti-PSA monoclonal antibodies. *Eur J Biochem,* 267**,** 4040-5.

WEINSTEIN, M. H., PARTIN, A. W., VELTRI, R. W. & EPSTEIN, J. I. 1996. Neuroendocrine differentiation in prostate cancer: enhanced prediction of progression after radical prostatectomy. *Hum Pathol,* 27**,** 683-7.

WU, C. & HUANG, J. 2007. Phosphatidylinositol 3-kinase-AKT-mammalian target of rapamycin pathway is essential for neuroendocrine differentiation of prostate cancer. *J Biol Chem,* 282**,** 3571-83.

YANG, Y., CHISHOLM, G. D. & HABIB, F. K. 1992. The distribution of PSA, cathepsin-D, and pS2 in BPH and cancer of the prostate. *Prostate,* 21**,** 201-8.

YUSIM, I., KRENAWI, M., MAZOR, E., NOVACK, V. & MABJEESH, N. J. 2020. The use of prostate specific antigen density to predict clinically significant prostate cancer. *Sci Rep,* 10**,** 20015.

ZHOU, C. K., CHECK, D. P., LORTET-TIEULENT, J., LAVERSANNE, M., JEMAL, A., FERLAY, J., BRAY, F., COOK, M. B. & DEVESA, S. S. 2016. Prostate cancer incidence

in 43 populations worldwide: An analysis of time trends overall and by age group. *Int J Cancer,* 138**,** 1388-400.
ZWEIG, M. H. & CAMPBELL, G. 1993. Receiver-operating characteristic (ROC) plots: a fundamental evaluation tool in clinical medicine. *Clin Chem,* 39**,** 561-77.

Figure Legends:

Figure 1: ZFPL1 gene expression in PC cells and its regulation.

A: The representative agarose gel shows the presence of amplified ZFPL1 mRNA following RT-qPCR reaction in several PC cell lines. B: Relative ZFPL1 mRNA abundance in PCa cell lines as measured by RT-qPCR. The ZFPL1 mRNA levels of PC3 cells were set at 1.0. C: Identification of ZFPL1 protein in prostate cells by western blot analysis. The position of the protein band of ZFPL1 immunoprecipitates in left lane was consistent with the expected molecular size of ZFPL1 (34.1 kDa). The right lane showed Dextran Blue molecular size markers (Bio-Rad Laboratories, Inc.). D: The bar graph presented the mean relative ZFPL1 mRNA abundance ± SEM (n=3) in LNCaP-C4 cells after treatment with CT (0, 5, 10, 50 and 100 nM). The control was set as 1.0. E: The bar graph revealed the mean relative ZFPL1 mRNA abundance ± SEM (n=3) in PC3-CTR cells after treatment with increasing concentrations of CT (0, 5, 10, 50 and 100 nm). F: The bar graph showed the dose-dependent increase in relative ZFPL1 mRNA abundance in LNCaP-C4 cells (mean ± SEM of n=3) in response to synthetic androgen R1881. $^{*}P<0.05$ and $^{**}P<0.0001$ (significantly different from the control, ordinary One-Way ANOVA and Tukey's multiple comparison test). ZFPL1, zinc finger protein like 1; PCa, prostate cancer; RT-qPCR, reverse transcription-quantitative PCR; CT, calcitonin.

Figure 2: Normalized accumulated ZFPL1 mRNA levels in primary prostate tissues.

Total mRNA was extracted from frozen primary prostate specimens. The mRNA was reverse transcribed and quantified by RT-qPCR. The ZFPL1 mRNA levels were normalized with GAPDH mRNA levels from same samples. The results are presented as relative ZFPL1 mRNA levels in prostate of different pathological status. Therese included normal, BPH and PCa of different Gleason score.

Figure 3: ZFPL1 expression in the primary PCa.

A: The photomicrographs showing specificity of *in situ* hybridization. A PC section was treated with sense ZFPL1 siRNA probe (A1) or antisense ZFPL1 siRNA probe (right). Only antisense probe hybridized with the PC specimen (A2). (Scale bar = 100 µm). B: The photomicrographs A3-A6 depict ZFPL1 mRNA expression in prostate sections of different cancer stages in comparison with non-cancer specimens (Scale bar = 50 µm). C: The photomicrographs on the left show H&E staining of human PC tissue sample, while those on the right show ZFPL1-immunopositive cells (green) and nuclear DAPI (Scale bar = 50 µm). White arrows point to the malignant areas contain

ZFPL1-immunopositive cells. D: The representative photomicrographs reveal the presence of ZFPL1-immunopostive cells (red) in a malignant prostate section, but not in its matched normal tissue (Scale bar = 50 µm). Nuclear stain is DAPI. The adjacent bar graph presents the mean percentage (n=6) of ZFPL1 immunopositive cells per field (magnification, x400) in PC vs. matched normal prostate tissue. *P<0.0001 (paired t-test). E: The representative photomicrographs reveal ZFPL1-immunopsitive cells (Red) and nuclear DAPI in different samples of a US Biomax PC tissue microarray (Scale bar = 50 µm). F: The bar graph presents the quantitated data of a PC tissue microarray (Figure 3D). The mean ± SEM (n=6) IHC index of each specimen in the microarray was calculated and plotted against the stage of PC. The mean IHC index of each cancer group except T1N0MO was significantly different from control. *P<0.005 (One Way ANOVA and Tukey's multiple comparison test). ZFPL1, zinc finger protein like 1; PC, prostate cancer; IHC, immunohistochemistry.

Figure 4: Co-localization of ZFPL1 with CgA and CD44 in the prostate.

A: The representative photomicrographs in upper panels show colocalization of ZFPL1 (green) and CgA (red) in PC3-CTR cells, and the lower panels show the same in primary PC specimens (Scale bar = 50 µm). B: The representative photomicrographs in upper panels show colocalization of ZFPL1(green) and CD44 in PC3-CTR cells, and the lower panels reveal the same in primary PC specimens (Scale bar = 50 µm). ZFPL1, zinc finger protein like 1; CgA, chromogranin A; PC, prostate cancer.

Figure 5: Subcellular localization of ZFPL1 in golgi bodies and exosomes of PCa cells.

A: Representative photomicrographs showed the colocalization of ZFPL1 (green) and CD81 (red, exosome marker) in PC3-CTR and LNCaP PCa cells (Scale bar = 25 µm). B: Representative photomicrographs revealed the colocalization of ZFPL1 (green) and CD63 (red, exosome/scretosome maker) (Scale bar = 25 µm). Cell borders were traced to show the location of exosomes with respect to a cell. Inset showed the magnified image (magnification, x1,000) of the location pointed by the arrow. C: Representative photomicrographs showed the colocalization of ZFPL1(green) and GM130 (red, Golgi body marker) (Scale bar = 25 µm). D: Representative immunoblot confirmed the presence of ZFPL1 in exosomes. This was demonstrated by co-precipitation of CD81 with ZFPL1 in the exosomal isolates of PC3-CTR and LNCaP-C4 PCa cells. □-actin is the loading control. ZFPL1, zinc finger protein like 1; PCa, prostate cancer.

Figure 6: Modulation of ZFPL1 expression in PC3-CTR and LNCaP-C4 prostate cancer cells. A: The immunoblots show the comparative efficacy of three siRNAs against ZFPL1 to suppress ZFPL1 protein levels in PC3-CTR and LNCaP-C4 cells by western blot analysis. β-actin was used as a housekeeping control. B: An immunoblot demonstrated that the transfection of ZFPL1 expression plasmid in PC3-CTR and LNCaP-C4 cells increased ZFPL1 protein levels in both cell lines. β-actin was used as a housekeeping control. ZFPL1, zinc finger protein like 1; si-, small interfering; ov, overexpression. *P<0.05.

Figure 7: ZFPL1 and PC cell proliferation and apoptosis.

A. The bar graph shows the inhibitory effect of ZFPL1 silencing on basal and CT-induced proliferation of PC-3CTR cells. The data are presented as the mean OD595 ± SEM (n=4)., *P<0.05 and ***P<0.0001 vs. the control receiving non-sense siRNA (unpaired t-test); ^^^P<0.0001 vs. +CT receiving non-sense siRNA (unpaired t-test).

B. The photomicrographs demonstrate the effect of either non-sense (control) or ZFPL1 siRNA ± CT on cleaved caspase 3 expression in LNCaP-C4 cells. The micrographs in the upper panel showed nuclear cleaved caspase 3 staining in untreated or CT-treated LNCaP-C4 cells, which received non-sense siRNA. A small number of cells were caspase 3-positive in control cells, but these declined when stimulated with CT suggesting CT attenuates caspase 3 activity. The micrographs in lower panels show the cells transfected with ZFPL1 siRNA in the absence/presence of CT. The results show a remarkable increasing in caspase 3 -positive cells with ZFPL1 silencing, however, the addition of CT reduced the effect of ZFPL1 silencing. C-D: The representative photomicrographs in first four pairs of micrographs showed the expression of cleaved caspase 3 (green) in LNCaP-C4 cells expressing carrier plasmid (upper panels) or ZFPL1 expression plasmid (Lower panels). The cells also received either vehicle, DEX (10 μM), CT (10 nM) or DEX + CT. DAPI stain was shown in Blue (Scale bar = 100 μm). As expected, DEX increased caspase 3-positive cells that was decreased by the addition of CT (upper four panels). Overexpression of ZFPL1 remarkably decreased caspase 3-positive cell population even in DEX-treated cells; CT further reduced the caspase 3-positive cells. These results suggest that ZFPL1 support cell proliferation and attenuate basal or DEX-induced apoptosis. CT produces similar effect.

C. The figure provides aggregate data of four experiments evaluating the effect of ZFPL1 knock-down on the number of cleaved caspase 3 positive (apoptotic) cells per 400X field. The ZFPl1 was

knocked down using siRNA1, siRNA2 and siRNA 3. The results are presented as mean ±SEM. *p<0.05 (One way ANOVA and Tukey's post-hoc test).

D. The figure provides aggregate data of four experiments testing the effect of ZFPL1 overexpression on the number of cleaved caspase 3 positive (apoptotic) cells per 400X field. The results are presented as mean ±SEM. *p<0.05 (One way ANOVA and Tukey's post-hoc test).

Figure 8: Effect of ZFPL1 knockdown/overexpression on invasion of PC cells.

A. The representative photomicrographs showed the effect of ±10 nM CT on invasiveness of PC3-CTR cells receiving either non-sense siRNA or ZFPL1 siRNA (1, 2 or 3) (Scale bar = 50 µm).

B. The representative photomicrographs showed the effect of ±10 nM CT on invasiveness of PC3-CTR cells overexpressing either vehicle Upper Panels) or ZFPL1 (Lower Panels).

C. The figure provides aggregate data of four invasion experiments testing the effect of ZFPL1 knock-down with siRNA1, siRNA2, siRNA3. The results are presented as mean ±SEM number of cells invaded per 400X field. *p<0.05 (One way ANOVA and Tukey's post-hoc test).

D. The figure provides aggregate data of four experiments testing the effect of ZFPL1 overexpression on the invasion of prostate cancer cells per 400X field. The results are presented as mean ±SEM number of cells per 400X field. *p<0.05 (One way ANOVA and Tukey's post-hoc test).

Figure 9: Effect of ZFPL1 knockdown on Akt phosphorylation. (A) The representative immunoblot on the left showed the effect of ±10 nM CT on p-Akt473 and p-Akt308 proteins in PC3-CTR cells receiving either non-sense (control) siRNA or ZFPL1 siRNA1, ZFPL siRNA2 or ZFPL1 siRNA3. Total Akt was used as a control protein. □-actin was used as the loading control. A representative immunoblot on the right showed the effect of ±10 nM CT on p-Akt473 and p-Akt308 proteins in LNCaP-C4 cells receiving either non-sense (control) siRNA or ZFPL1 siRNA1, ZFPL siRNA2 or ZFPL1 siRNA3. Akt was used as a control protein. β-actin provided the loading control. (B) A representative immunoblot showed the effect of ± 10 nM CT on p-Akt473 and p-Akt308 proteins in LNCaP-C4 cells transfected with either carrier plasmid or ZFPL1 expression plasmid, respectively. Akt was used as a control protein. (C) A representative immunoblot on the right showed the effect of ±10 nM CT on pAkt473 and pAkt308 proteins in LNCaP-C4 cells transfected with either carrier plasmid or ZFPL1 expression plasmid respectively. Akt was used as a control protein. β-actin was used as the loading control.

Figure 10. Plasma NEM and PSA levels in normals, BPH, PCa and other Ca groups. Box

and Whisker plots for NEM and PSA that shows the summary and distribution of plasma NEM and PSA levels in our cohort of 508 patients that was divided in four groups: N=normals, (n=98), BPH (n=19), PCa (n=311), and other Ca (n=80). The data was statistically analyzed by Kruskal-Wallis test to examine the significance among ranks of all four groups. Both biomarkers displayed significant differences between PCa group vs all other groups. The data was also analyzed by one way ANOVA multiple comparison. One way ANOVA showed significant differences between NEM levels of PCa group vs other three groups. However, no significant differences were found in plasma PSA levels between these groups. ** $p<0.05$.

Figure 11. Receiver Operatic Curves (ROC) analysis of NEM and PSA. The curves were derived by Prism (8.0) after entering the data of plasma levels of both biomarkers of the cohort consisting of normals (n=98) and PCa (n=311). The area under the curve (AUC) for NEM (black) was 0.9935±0.0034 ($p<0.0001$). The AUC for the PSA (blue) was 0.8140±0.0209 ($p<0.0001$).

Figure 12. Scattergrams of plasma NEM and PSA levels in cohort of patients showing PSA levels between 4-10 ng. A: Scattergrams of plasma NEM and PSA levels in patients diagnosed as BPH (n=19); B: Scattergrams of plasma NEM and PSA levels in patients displaying plasma PSA levels in the range of 4-10 ng/ml irrespective of their clinical status (n=135).

Figure 13. Bar graphs of plasma NEM and PSA levels in different stages of PCa. Figure 3A: A bar graph showing mean±SEM of plasma NEM levels in different tumor stage. The cohort consisted of stage 1 (n=100); stage 2 (n=89); stage 3 (n=57) and stage 4 (n=4). Figure 3B: A bar graph showing mean±SEM of plasma PSA levels in different tumor stage. The cohort consisted of stage 1 (n=100); stage 2 (n=89); stage 3 (n=57) and stage 4 (n=4).

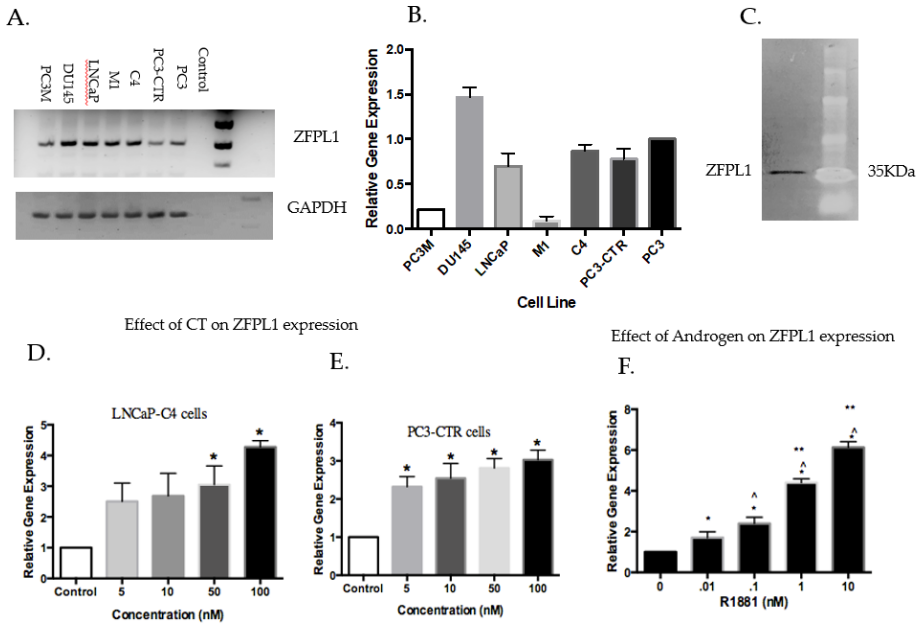

Figure 1

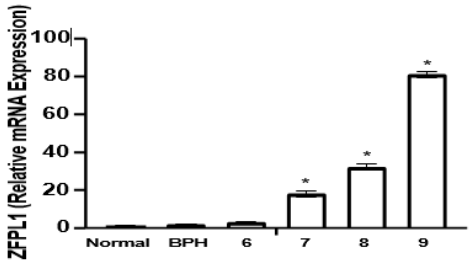

Figure 2

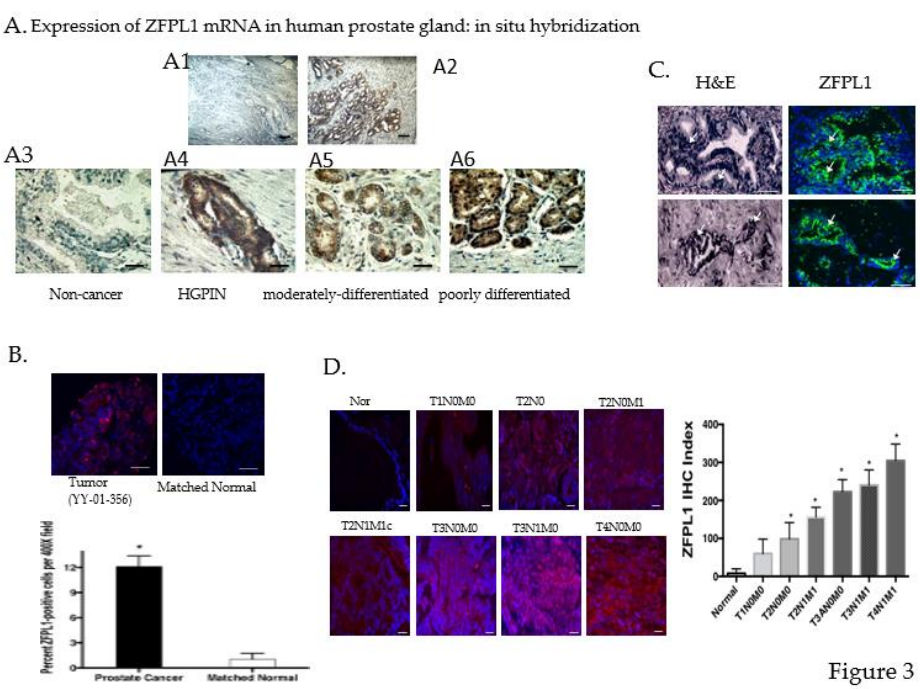

Figure 3

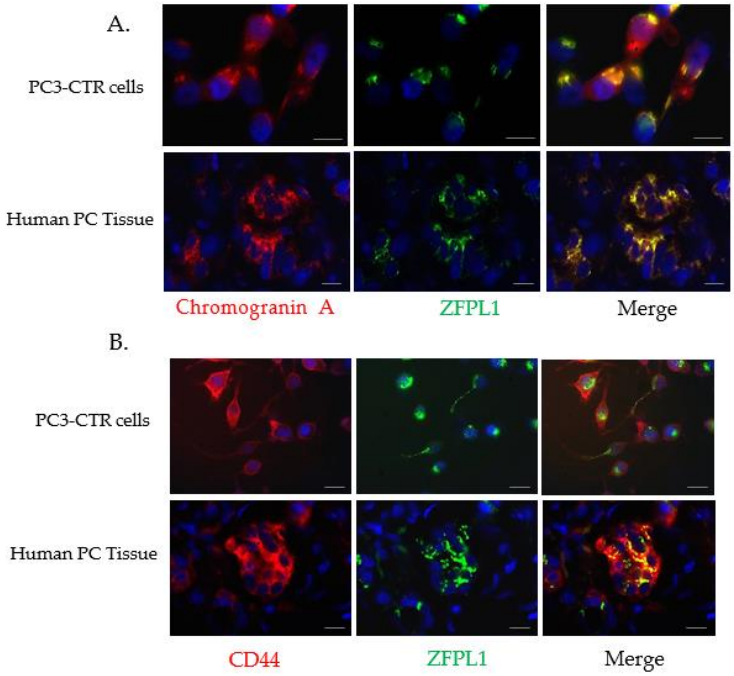

Figure 4

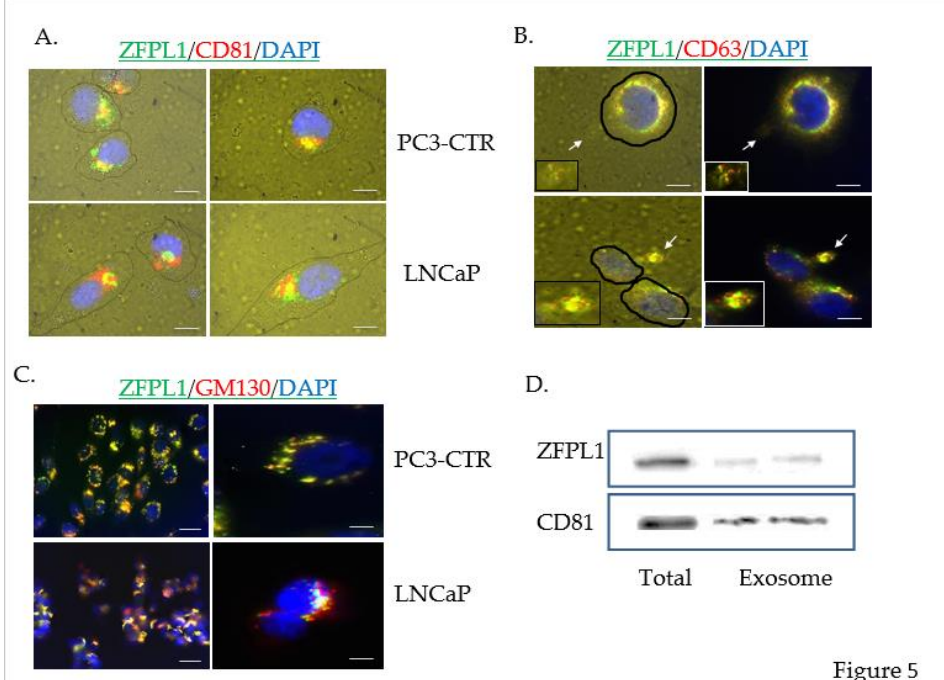

Figure 5

A.

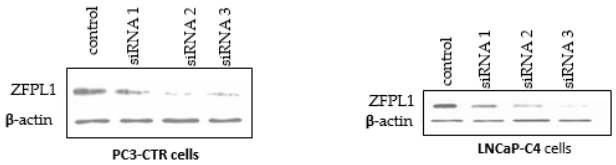

B.

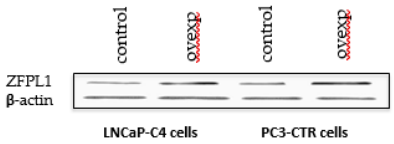

Figure 6

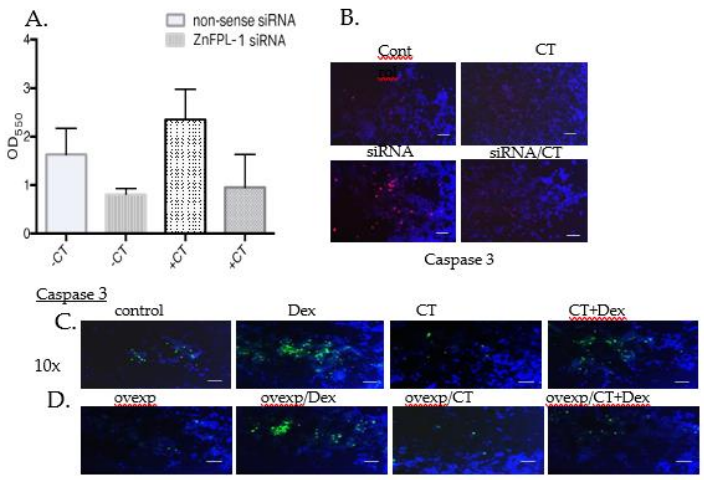

Figure 7

Figure 7

C.

Effect of ZFPL1 knock-down on apoptosis

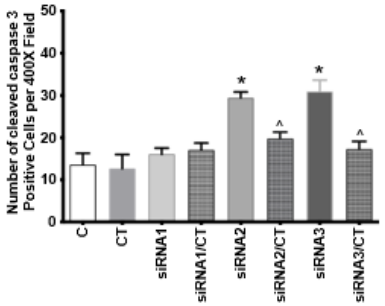

D.

Effect of ZFPL1 overexpression on apoptosis

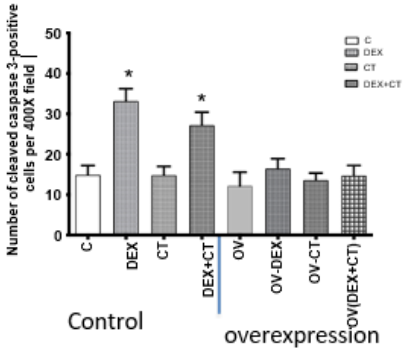

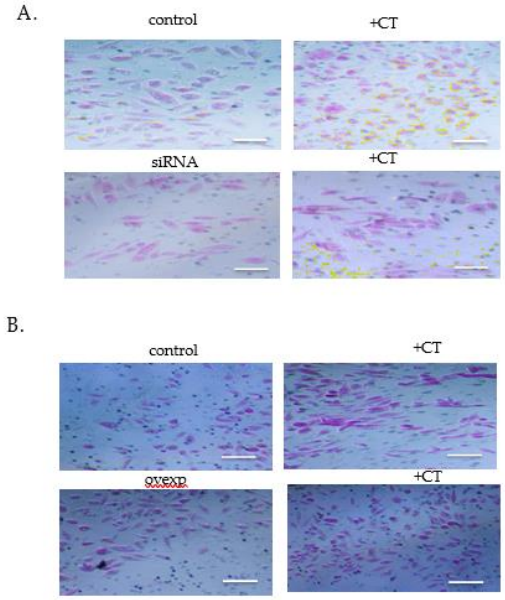

Figure 8

C. ZFPL1 knock-down and invasion D. ZFPL1 overexpression and invasion

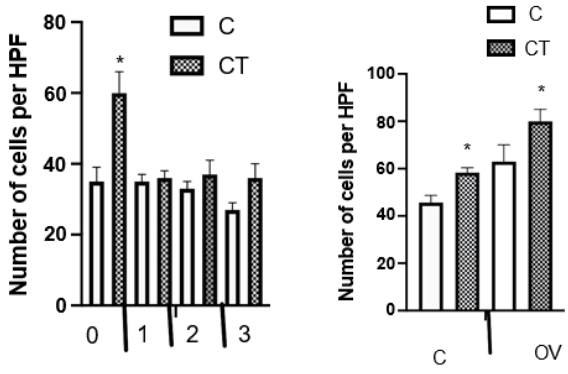

Figure 8

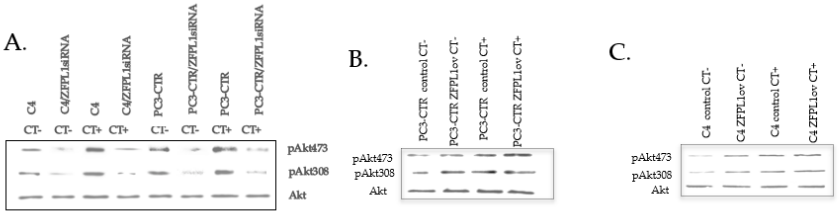

Figure 9

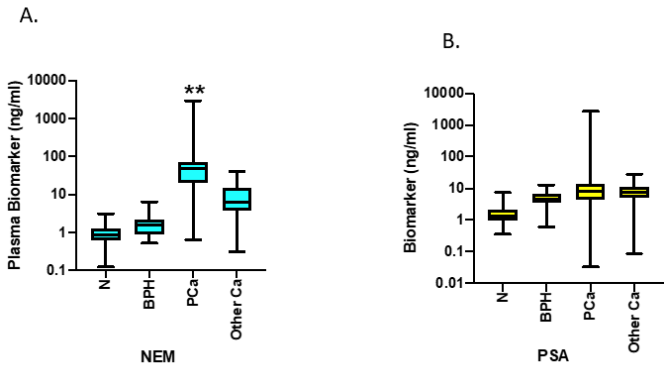

Figure 10

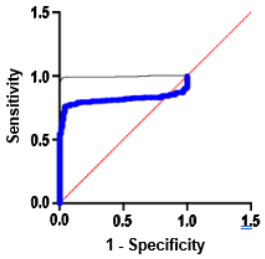

Figure 11

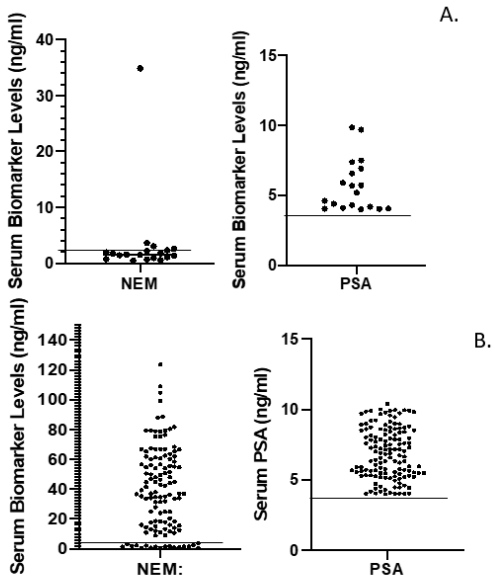

Figure 12

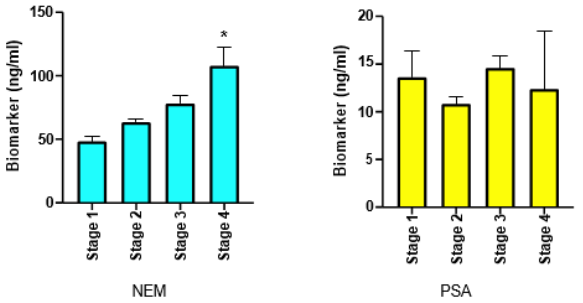

Number of Subjects (n)	Average Age (years)	Age Range (years)	Tumor Stage
11 (LSUHSC, individuals)	60.82	48-71	Stage I
89 (LSU, individuals)	61.16	48-75	Stage II
57 (LSUHSC, individuals)	62.26	48-75	Stage III
4 (LSUHSC)	59.67	54-62	Stage IV

Figure 13

Table 1. **CT induced genes**

No.	Name of identified gene	Abbreviation	Signal strength
1	Immunoglobulin Heavy Constant Gamma 1	IGHG1	+
2	Calpain 2	CAPN2	++
3	S100 Calcium Binding Protein A11	S100A11	+
4	F-Box Protein 2	FBXO2	+++
5	Zinc Finger Protein Like 1	ZFPL1	++++
6	ZFP36 Ring Finger Protein Like 1	ZFP36L1	+++
7	Immunoglobulin Heavy Variable 4-31	IGHV431	+
8	Branched Chain Ketoacid Dehydrogenase Kinase	BCKDK	+
9	Butyrophilin Subfamily 2 Member A2	BTN2A2	++

Differentially expressed genes identified from the gene BLAST program that were CT induced and had homology to human gene sequences

Table 2. **Presence of ZFPL1 in the prostate cancer**

	Benign Acini	HGPIN Acini	PC (Gleason: 1-6)	PC (Gleason: 7-10)
Number of cases	23	11	21	23
Mean ± SEM	13.51 ± 3.01	39.73 ± 3.17*	47.13 ± 4.95*	93.25 ± 3.83**

Tabulated representation of human prostate tissue samples from non-cancer control to different prostate cancer stages and related ZFPL1 mRNA expression by using in-situ hybridization

Table 3: Biomarker Performance

Biomarker	Accuracy	PPV	NPV	Subjects (n)
NEM (normal+PCa)	0.933	0.982	0.993	311+98
PSA (normal+PCa)	0.880	0.965	0.719	311+98
NEM (BPH+PCa)	0.981	0.925	0.981	311+19
PSA (BPH+PCa)	0.821	0.821	0.331	311+19